Calcium-independent Phospholipase A₂γ Enhances Activation of the ATF6 Transcription Factor during Endoplasmic Reticulum Stress*

Hanan Elimam, Joan Papillon, Tomoko Takano[1], and Andrey V. Cybulsky[2]
From the Department of Medicine, McGill University Health Centre, McGill University, Montreal, Quebec H3A 1A1, Canada

Background: Calcium-independent $PLA_2\gamma$ (i$PLA_2\gamma$) is a membrane-bound enzyme that localizes at the endoplasmic reticulum (ER).
Results: i$PLA_2\gamma$ amplified activation of the ATF6 pathway of the unfolded protein response, resulting in up-regulation of ER chaperones and cytoprotection.
Conclusion: i$PLA_2\gamma$ enhances activation of ATF6.
Significance: Modulating i$PLA_2\gamma$ activity may provide opportunities for pharmacological intervention in glomerular diseases associated with ER stress.

Injury of visceral glomerular epithelial cells (GECs) causes proteinuria in many glomerular diseases. We reported previously that calcium-independent phospholipase $A_2\gamma$ (i$PLA_2\gamma$) is cytoprotective against complement-mediated GEC injury. Because i$PLA_2\gamma$ is localized at the endoplasmic reticulum (ER), this study addressed whether the cytoprotective effect of i$PLA_2\gamma$ involves the ER stress unfolded protein response (UPR). In cultured rat GECs, overexpression of the full-length i$PLA_2\gamma$, but not a mutant i$PLA_2\gamma$ that fails to associate with the ER, augmented tunicamycin-induced activation of activating transcription factor-6 (ATF6) and induction of the ER chaperones, glucose-regulated protein 94 (GRP94) and glucose-regulated protein 78 (GRP78). Augmented responses were inhibited by the i$PLA_2\gamma$ inhibitor, (R)-bromoenol lactone, but not by the cyclooxygenase inhibitor, indomethacin. Tunicamycin-induced cytotoxicity was reduced in GECs expressing i$PLA_2\gamma$, and the cytoprotection was reversed by dominant-negative ATF6. GECs from i$PLA_2\gamma$ knock-out mice showed blunted ATF6 activation and chaperone up-regulation in response to tunicamycin. Unlike ATF6, the two other UPR pathways, *i.e.* inositol-requiring enzyme 1α and protein kinase RNA-like ER kinase pathways, were not affected by i$PLA_2\gamma$. Thus, in GECs, i$PLA_2\gamma$ amplified activation of the ATF6 pathway of the UPR, resulting in up-regulation of ER chaperones and cytoprotection. These effects were dependent on i$PLA_2\gamma$ catalytic activity and association with the ER but not on prostanoids. Modulating i$PLA_2\gamma$ activity may provide oppor-

tunities for pharmacological intervention in glomerular diseases associated with ER stress.

Phospholipase A_2 (PLA_2)[3] comprises a family of enzymes that play important roles in numerous cellular processes. PLA_2s hydrolyze the acyl bond at the *sn*-2 position of phospholipids to yield free fatty acids, such as arachidonic acid and lysophospholipids (1, 2). Both products represent precursors for signaling molecules that can exert multiple biological functions, in particular, arachidonic acid can be converted into bioactive eicosanoids by cyclooxygenases, lipoxygenases, and cytochrome P450 proteins (3). Calcium-independent $PLA_2\gamma$ (i$PLA_2\gamma$) is a membrane-bound enzyme that is reported to localize at the endoplasmic reticulum (ER), peroxisomes, and mitochondria (4). These distinct sites of localization are likely dependent on specific domains in the N terminus of the enzyme (5). In renal proximal tubular cells, i$PLA_2\gamma$ removes oxidized phospholipids from the ER membrane during oxidative stress; thus, i$PLA_2\gamma$ may act to repair damaged lipids or prevent lipid peroxidation during oxidative stress (4). Consistent with these results, i$PLA_2\gamma$ knockdown in renal cells increased lipid peroxidation and induced apoptosis (6). Conversely, inhibition of microsomal i$PLA_2\gamma$ in rabbit renal proximal tubular cells during cis-platin-induced apoptosis reduced apoptosis markers, indicating that i$PLA_2\gamma$ contributes to apoptosis (7). Mitochondrial i$PLA_2\gamma$ has been also shown to actively participate in the permeability transition pore opening of the mitochondria and the release of the proapoptotic cytochrome *c* (8). i$PLA_2\gamma$ knock-out mice demonstrate multiple bioenergetic dysfunctional phenotypes (9), although they are resistant to obesity and show less insulin resistance (10). Thus, the biological functions of i$PLA_2\gamma$

[1] To whom correspondence may be addressed: Division of Nephrology, McGill University, 3775 University St., Rm. 236, Montreal, Quebec H3A 2B4, Canada. Tel.: 1-514-398-2171; Fax: 1-514-843-2815; E-mail: tomoko.takano@mcgill.ca.
[2] To whom correspondence may be addressed: Division of Nephrology, Royal Victoria Hospital, 687 Pine Ave. West, Montreal, Quebec H3A 1A1, Canada. Tel.: 1-514-398-8148; Fax: 1-514-843-2815; E-mail: andrey.cybulsky@mcgill.ca.

in the context of cell injury are complex and appear to be cell/context-dependent.

Glomerular visceral epithelial cells (GECs) or podocytes are intrinsic components of the kidney glomerulus and play a key role in the maintenance of glomerular permselectivity. Various forms of glomerulonephritis are associated with podocyte injury, which leads to impaired glomerular permselectivity (proteinuria). We reported previously that complement C5b-9 activates iPLA$_2$γ in GECs in a protein kinase-dependent manner (11) and that overexpression of iPLA$_2$γ is protective against complement-dependent GEC injury (12). In GECs, iPLA$_2$γ is localized at the ER and mitochondria, and this localization is dependent on the N-terminal region of iPLA$_2$γ (11). The isoform of iPLA$_2$γ that lacks the N-terminal region is misplaced from the ER and fails to produce prostaglandin E$_2$ in response to complement, although its activity is similar to the full-length isoform when tested *in vitro*. Thus, it appears that one of the major sites of iPLA$_2$γ activation in GECs is the ER; however, physiological functions of iPLA$_2$γ at the ER have not been well delineated.

In the ER, proteins are properly folded and are then transported to the Golgi apparatus, whereas misfolded proteins undergo ER-associated degradation (13). When the amount of misfolded proteins in the ER exceeds the capacity of the folding apparatus and ER-associated degradation machinery, the misfolded proteins lead to ER stress and activation of the unfolded protein response (UPR) (14–17). There are three major UPR pathways, namely activating transcription factor-6 (ATF6), inositol-requiring enzyme 1α (IRE1α), and protein kinase RNA-like ER kinase (PERK) pathways (14, 16, 18). Accumulation of misfolded proteins leads to release of ATF6 from the ER and translocation to the Golgi, where it is cleaved by the site-1 and site-2 proteases. The cleaved cytosolic fragment of ATF6, which has a DNA-binding domain, migrates to the nucleus to activate transcription of ER chaperones, including glucose-regulated protein 94 (GRP94) and glucose-regulated protein 78 (GRP78), which in turn enhance ER protein folding capacity and limit cytotoxicity. The IRE1α endoribonuclease cleaves X box-binding protein-1 (*xbp1*) mRNA and changes the reading frame to yield a potent transcriptional activator, which works in parallel with ATF6 to activate transcription of ER chaperones genes. PERK phosphorylates the eukaryotic translation initiation factor-2α subunit (eIF2α), which reduces the general rate of translation and aims at decreasing the protein load on a damaged ER. The three UPR pathways are often activated together, but selective activation of some pathways together with suppression of others can occur (16, 19).

The goal of this study was to address the mechanisms of cytoprotection by iPLA$_2$γ in GECs. Because iPLA$_2$γ is localized at the ER in GECs, we studied whether cytoprotection by iPLA$_2$γ involves the UPR pathways. We demonstrate that in GECs, iPLA$_2$γ amplifies tunicamycin-induced ATF6 activation and up-regulation of ER chaperones, which limits cell injury.

EXPERIMENTAL PROCEDURES

Materials—Tissue culture media and Lipofectamine 2000 were from Invitrogen. Electrophoresis reagents were from Bio-Rad. Mouse monoclonal anti-green fluorescent protein (GFP) and rat anti-GRP94 antibodies were from Santa Cruz Biotechnology (Santa Cruz, CA). Rabbit anti-GRP78 (BiP) antibody was from Enzo Life Sciences (Farmingdale, NY). Rabbit anti-phospho-eIF2α (Ser[51]) was purchased from New England Biolabs (Mississauga, Ontario, Canada). Rabbit monoclonal anti-actin antibody, tunicamycin, thapsigargin, and U18666A were from Sigma. Enhanced chemiluminescence (ECL) reagents were from GE Healthcare. (*R*)-Bromoenol lactone (R-BEL) was from Cayman Chemical (Ann Arbor, MI). Wild type (WT), M4, and S511A/S515A GFP-iPLA$_2$γ cDNAs were described previously (11). Plasmids 5xATF6-GL3, pCGN-ATF6(1–373)m1, and low density lipoprotein receptor (LDLR) promoter-luciferase were from Addgene (Cambridge, MA) (20, 21). A retroviral construct consisting of the SV40 large T antigen gene containing both the tsA58 and the U19 mutations was kindly provided by Prof. Parmjit Jat (Ludwig Institute for Cancer Research, London, UK) (22).

Cell Culture and Transfection—Rat GECs were derived from glomerular explants, and the methods for culture and characterization have been described previously (11, 12, 23). GECs were maintained in K1 medium on plastic substratum. Rat GECs stably transfected with GFP-iPLA$_2$γ and control GECs were described previously (11). 293T and COS-1 cells were cultured in Dulbecco's modified Eagle's medium (DMEM) supplemented with 10% fetal bovine serum. Transient transfection of GECs or COS-1 cells was performed using Lipofectamine 2000.

iPLA$_2$γ knock-out (KO) mice were kindly provided by Dr. Richard Gross (Washington University, St. Louis, MO) (24). Mouse GECs were derived from iPLA$_2$γ KO mice and WT control. Briefly, glomeruli were isolated from both KO and WT mice by differential sieving, as described previously (25). The purity of glomeruli obtained from the isolation was consistently ~70–80%. Isolated glomeruli were seeded on type I collagen-coated culture dishes for 5 days in K1 medium (11). A week after the first epithelial cell outgrowth, the cells were immortalized by infection with retrovirus carrying the temperature-sensitive SV40 large T antigen, which was performed by adding retrovirus-containing supernatants from 293T packaging cells (22, 26). Selection was carried out with puromycin, and colonies were isolated using cloning rings. Then the cells were allowed to grow for 2 additional weeks under permissive conditions (33 °C). More than 98% of cells showed morphological characteristics of GECs. By immunofluorescence microscopy (method below), both cell lines displayed positive staining for synaptopodin and nephrin at both permissive (33 °C) and nonpermissive (37 °C) temperatures (Fig. 1*A*). These results confirm that the cells are of podocyte origin, although they are distinct from certain other GEC lines, where expression of synaptopodin was reported only at the nonpermissive temperature (25, 27).

Reverse transcription-polymerase chain reaction (RT-PCR; method below) confirmed the absence of iPLA$_2$γ mRNA expression in cells from KO mice (Fig. 1, *B* and *C*). In addition, quantitative RT-PCR (see below) was performed to measure expression of iPLA$_2$γ mRNA isoforms in cultured GEC lines (Table 1). We were not able to compare the level of iPLA$_2$γ protein expression, because we could not identify an antibody that reacts with endogenous iPLA$_2$γ protein reliably.
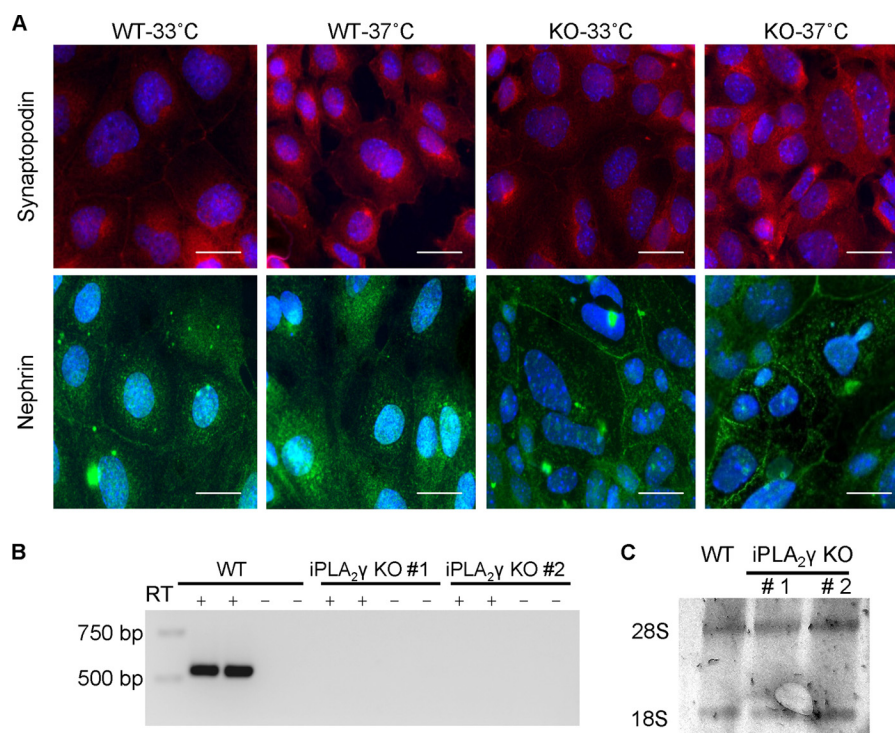
FIGURE 1. **Characterization of iPLA$_2\gamma$ KO mouse GECs.** *A,* immunofluorescence staining for podocyte-specific proteins. GECs were cultured on glass coverslips for 24 h and were then stained for synaptopodin and nephrin. WT and iPLA$_2\gamma$ KO GECs displayed positive staining for synaptopodin at the permissive temperature (33 °C). The staining appeared stronger at the nonpermissive temperature (37 °C), particularly in the cytoplasm and extending into cell processes. Expression of nephrin was visualized as a punctate cell surface and cytoplasmic staining. Nephrin was expressed at both permissive (33 °C) and nonpermissive (37 °C) temperatures in both cell lines. *Bars,* 20 μm. *B,* expression of endogenous iPLA$_2\gamma$ mRNA in mouse GECs was assessed by RT-PCR. WT mouse GECs express iPLA$_2\gamma$ mRNA. iPLA$_2\gamma$ KO #1 and KO #2 cell lines (two different clones of mouse GECs), do not show any iPLA$_2\gamma$ mRNA. Control lanes (−) were devoid of RT. *C,* 28 S and 18 S ribosomal RNAs were visualized by staining with ethidium bromide and demonstrate equal loading.

TABLE 1
Expression of iPLA$_2\gamma$ mRNAs in GEC lines

Total RNA was extracted from GECs (and mouse glomeruli for comparison). RNA was reverse-transcribed and amplified using quantitative PCR. In the GECs transfected with full-length (M1) GFP-iPLA$_2\gamma$ WT or M4 GFP-iPLA$_2\gamma$, RNA was extracted 24 h after transfection. Relative quantification (RQ) is presented as an average of 3–6 values.

Cell type	RQ
Untransfected rat GECs	1.0
M1 GFP-iPLA$_2\gamma$ WT-rat GECs	17.9
M4 GFP-iPLA$_2\gamma$-rat GECs	16.8
WT mouse GECs	0.5
iPLA$_2\gamma$ KO mouse GECs	0
WT mouse glomeruli	1.6

Immunofluorescence Microscopy—Cells were cultured on glass coverslips for 24 h. All incubations were carried out at 22 °C. To examine the expression of nephrin and synaptopodin, cells were fixed with 3% paraformaldehyde in PBS for 15 min and were permeabilized with 0.1% Triton X-100 in PBS for 30 min. After washing with PBS, cells were incubated with rabbit anti-nephrin antiserum, rabbit anti-synaptopodin antibody, or nonimmune rabbit serum (negative control) diluted in 3% BSA for 2 h. Cells were washed and incubated with fluoresceinated goat anti-rabbit IgG in 3% BSA for 30 min. Nuclei were counterstained with 4'6-diamidino-2-phenylindole (DAPI, 30 nM) in PBS for 4–5 min just before mounting the coverslips onto glass slides. Staining was visualized with a Zeiss AxioObserver fluorescence microscope with visual output connected to an AxioCam digital camera.

RT-PCR—For the analysis of iPLA$_2\gamma$ mRNA expression, total RNA was extracted from iPLA$_2\gamma$ KO and WT immortalized mouse GECs using the RNeasy mini kit (Qiagen). cDNA synthesis was performed by QuantiTect reverse transcriptase (Invitrogen). The RT step was omitted in negative controls. PCR for iPLA$_2\gamma$ was done using mouse iPLA$_2\gamma$ sequence-specific primers as follows: forward 5'-ATTGATGGTGGAGGA-ACAAGA-3' and reverse 5'-ATGGCCTGCCACATTTTA-TAC-3'. PCR consisted of 23 cycles (95 °C for 30 s; 62 °C for 30 s; and 72 °C for 105 s (but 10 min in the final cycle)) and was carried out with *Taq* DNA polymerase. PCR products were analyzed on 2% agarose gels after staining with ethidium bromide.

For analysis of *xbp1* mRNA splicing, total RNA was extracted from GECs and reverse-transcribed as above. To amplify *xbp1* mRNA, the primers uses were as follows: forward 5'-AACTC-CAGCTAGAAAATCAGC-3' and reverse 5'-CCATGGGAA-GATGTTCTGGG-3'. PCR consisted of 25 cycles (95 °C for 30 s; 58 °C for 30 s; and 72 °C for 1 min (but 10 min in the final cycle)) and was carried out with *Taq* DNA polymerase. *xbp1* products were visualized on agarose gels, as 530- and 556-bp fragments representing spliced (*xbp1*$_S$) and unspliced (*xbp1*$_U$) xbp1.

Quantitative Real Time PCR—Total RNA was prepared from GECs and glomeruli using TRIzol reagent (Invitrogen) and was reverse-transcribed as above. The PCR for iPLA$_2\gamma$ was done using rat, mouse, and human iPLA$_2\gamma$ sequence-specific primers as follows: forward 5'-CCTGAAGGAAAAGGAGTGG-3' and

reverse 5′-CTTGTTCCTCCACCATCAAT-3′. Real time PCRs were performed on an ABI 7300 sequence detection system (Applied Biosystems, Foster City, CA), and amplified DNA was detected by SYBR Green incorporation. Values were normalized to hypoxanthine-guanine phosphoribosyltransferase or glyceraldehyde-3-phosphate dehydrogenase mRNA levels in the same sample.

Dual-Luciferase Reporter Assay—Cells were transiently transfected with empty vector or iPLA$_2$γ, together with a firefly luciferase reporter cDNA and a cDNA-encoding *Renilla* luciferase, using Lipofectamine 2000. Cells were cultured for 24 h and then stimulated with tunicamycin (0.1 μg/ml, 18 h). Lysates were assayed for firefly and *Renilla* luciferase activities using a kit (Dual-Luciferase^{TM} reporter assay system, Promega, Madison, WI), according to manufacturer's instructions. Measurements were performed in a Lumat LB 9507 luminometer (Berthold, Oak Ridge, TN), and the ratios between firefly and *Renilla* luciferase activities (the latter a marker of transfection efficiency) were calculated. Results are presented in relative luminescence units.

Immunoblotting—Cells were lysed in ice-cold buffer containing 1% Triton X-100, 125 mM NaCl, 10 mM Tris, pH 7.4, 1 mM EGTA, 2 mM Na$_3$VO$_4$, 10 mM sodium pyrophosphate, 25 mM NaF, and protease inhibitor mixture (Roche Diagnostics). Equal amounts of lysate proteins were dissolved in Laemmli buffer and were subjected to SDS-PAGE under reducing conditions. Proteins were then electrophoretically transferred onto a nitrocellulose membrane and blocked at room temperature for 1 h with 5% dry milk in buffer containing 10 mM Tris, pH 7.5, 50 mM NaCl, 2.5 mM EDTA, and 0.05% Tween 20. The membrane was then incubated with primary and secondary antibodies and developed with ECL.

Assay for Tunicamycin-induced Cell Death—Tunicamycin-induced cell death was determined by measuring lactate dehydrogenase (LDH) release, as described previously (28). Briefly, cells were cultured in a 24-well plate for 48 h. DNA transfection (when required) was performed 24 h after plating. Cells were then treated with 1–10 μg/ml tunicamycin for 24 h. At the end of the incubation, cell supernatants were collected, and the cells adherent to the culture dishes were lysed with 1% Triton X-100. Then both cell supernatants and Triton lysates were analyzed for LDH activity by adding NAD in glycine/lactate buffer. LDH converts lactate and NAD to pyruvate and NADH. The rate of increase in the absorbance at 340 nm, due to formation of NADH, represents LDH activity. Specific release of LDH release was calculated as supernatant/(supernatant + lysate) × 100.

Statistics—Data are presented as mean ± S.E. One-way analysis of variance was used to determine significant differences among groups. When significant differences were found, individual comparisons were made between groups using the Student's *t* test and adjusting the critical value according to Bonferroni's method.

RESULTS

iPLA$_2$γ Amplifies the Activation of ATF6—Previous studies demonstrated that complement activates iPLA$_2$γ and that the iPLA$_2$γ pathway restricts complement-induced cytotoxicity in GECs (11, 12). Given that iPLA$_2$γ is, in part, localized at the ER, we hypothesized that the cytoprotective actions of iPLA$_2$γ may involve the UPR. First, we addressed the activation of ATF6, by employing a reporter construct containing five tandem copies of an ATF6-response element fused to firefly luciferase (p5xATF6-GL3) (20). GECs were co-transfected with full-length (M1) GFP-iPLA$_2$γ (or empty vector in control) and the ATF6 luciferase reporter. (In a previous study, we showed that the enzymatic activity of GFP-iPLA$_2$γ was comparable with untagged iPLA$_2$γ (11).) Cells were then treated for 18 h with the *N*-linked glycosylation inhibitor, tunicamycin, which causes accumulation of misfolded proteins in the ER and is a potent inducer of ER stress (15). In vector-transfected control cells, tunicamycin stimulated ATF6 reporter activity, and this was augmented significantly by iPLA$_2$γ (Fig. 2*A*). In contrast, an N-terminally truncated form of iPLA$_2$γ (M4 iPLA$_2$γ), which does not associate with the ER (11), failed to augment tunicamycin-induced ATF6 activation, implying that the association with the ER is required for ATF6 activation (Fig. 2*A*). Expression of M1 and M4 iPLA$_2$γ was confirmed by immunoblotting (Fig. 2*B*). Both the tunicamycin-stimulated and the iPLA$_2$γ-amplified ATF6 activities were inhibited by the iPLA$_2$γ inhibitor, R-BEL, but not by indomethacin, an inhibitor of cyclooxygenases (Fig. 2*C*), suggesting that the tunicamycin-induced activation of the ATF6 reporter is dependent on endogenous and overexpressed iPLA$_2$γ catalytic activity but not prostanoids. An analogous experiment was performed using different ER stressors, including thapsigargin, a potent inhibitor of the endoplasmic reticulum Ca^{2+}-ATPase (29), and DTT, a reducing agent, which prevents formation of disulfide bonds between cysteine residues of proteins, thereby inducing protein misfolding and ER stress (30). Similar to tunicamycin, thapsigargin and DTT stimulated ATF6 reporter activity, and iPLA$_2$γ amplified their effects (Fig. 2*D*). To substantiate the conclusion that endogenous iPLA$_2$γ can also modulate the ATF6 pathway, we employed GECs derived from WT and iPLA$_2$γ KO mice. The tunicamycin-induced activation of the ATF6 reporter was reduced in iPLA$_2$γ KO GECs, compared with WT (Fig. 3*A*). Thus, both endogenous and ectopically overexpressed iPLA$_2$γ contribute to the activation of the ATF6 pathway of the UPR in GECs.

iPLA$_2$γ Amplifies the Induction of ER Chaperones—In mammalian cells, the up-regulation of ER chaperones, including GRP94 and GRP78 (BiP), is believed to be due mainly to the activation of ATF6. Because iPLA$_2$γ amplified the effect of tunicamycin on ATF6 activation, we proceeded to investigate whether this effect on ATF6 activation was associated with up-regulation of ER chaperones. First, it should be noted that cDNA transfection did not independently stimulate increases in GRP94 and GRP78, *i.e.* there were no significant differences between untransfected and vector-transfected cells (Fig. 4). Brief incubation of GECs overexpressing iPLA$_2$γ with tunicamycin (10 μg/ml, 6 h) did not induce significant increases in GRP94 and GRP78 expression, compared with vector-transfected cells (results not shown). In contrast, incubation of untransfected or vector-transfected GECs with tunicamycin (5 or 10 μg/ml) for 18 h induced modest increases in the expression of GRP94 and GRP78, and this effect was amplified by
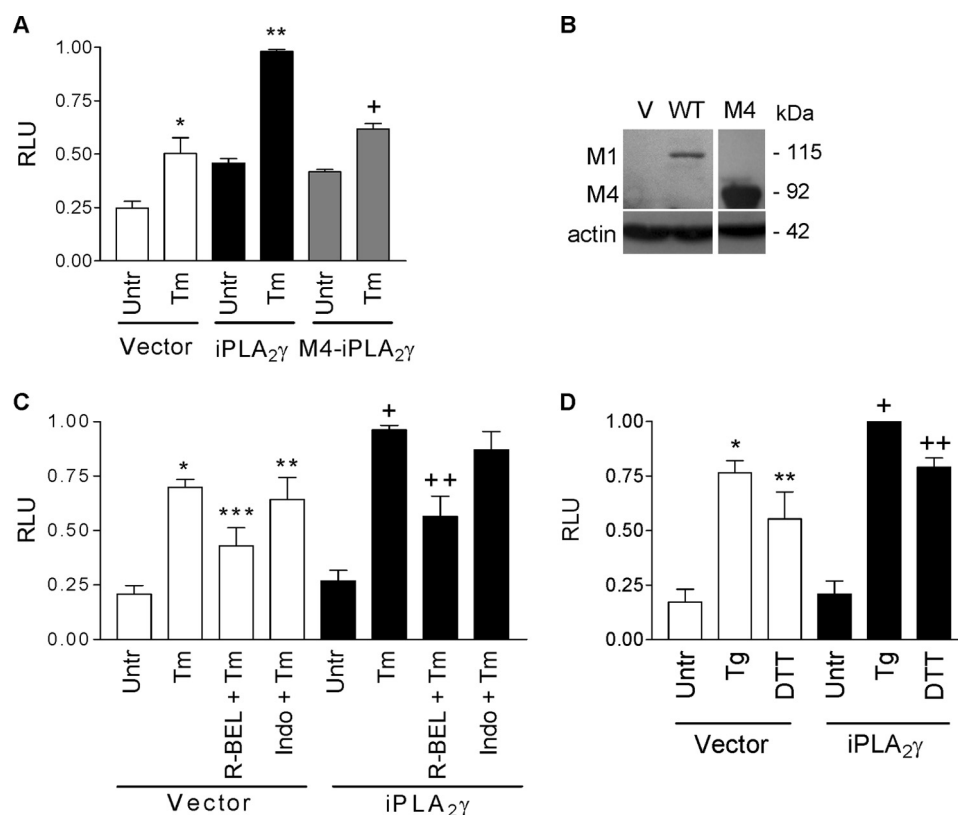
FIGURE 2. **iPLA$_2\gamma$ amplifies tunicamycin-induced ATF6 luciferase-reporter activity.** *A,* rat GECs were transiently co-transfected with full-length (M1) GFP-iPLA$_2\gamma$, N-terminal truncated (M4) GFP-iPLA$_2\gamma$, or vector (control), plus ATF6 firefly luciferase-reporter and *Renilla* luciferase. After 24 h, cells were untreated (*Untr*) or incubated with tunicamycin (*Tm*, 0.1 μg/ml, 18 h). Tunicamycin stimulated ATF6 reporter activity (expressed in relative luminescence units (*RLU*)), and iPLA$_2\gamma$ amplified the effect of Tm. *, $p < 0.001$ Tm *versus* untreated (*Vector*); **, $p < 0.001$ iPLA$_2\gamma$ *versus* vector (Tm) and *versus* M4 iPLA$_2\gamma$ (Tm); +, $p < 0.01$ Tm *versus* untreated (M4 iPLA$_2\gamma$), three experiments performed in triplicate. *B,* representative anti-GFP antibody immunoblots showing expression of full-length (M1) WT and N-terminal truncated (M4) GFP-iPLA$_2\gamma$ (*V*, vector transfection). *C,* rat GECs were transiently co-transfected as in *A*. After 24 h, cells were untreated (*Untr*), incubated with tunicamycin (*Tm*, 0.1 μg/ml, 18 h), or preincubated with R-BEL (5 μM, 30 min) or indomethacin (10 μM, 30 min) before treatment with Tm. Tunicamycin stimulated ATF6-reporter activity, and iPLA$_2\gamma$ amplified the effect of Tm. The amplified ATF6 activity was inhibited by R-BEL but not by indomethacin. *, $p < 0.001$ Tm *versus* untreated (*Vector*); **, $p < 0.01$ Tm + indomethacin (*Indo*) *versus* untreated (*Vector*); ***, $p < 0.05$ R-BEL + Tm *versus* Tm (*Vector*); +, $p < 0.05$ iPLA$_2\gamma$ *versus* vector (Tm); ++, $p < 0.001$ R-BEL + Tm *versus* Tm (iPLA$_2\gamma$), five experiments performed in triplicate. *D,* GECs were co-transfected as in *A*. Cells were untreated or incubated with thapsigargin (*Tg*, 0.5 μM, 18 h) or DTT (0.5 μM, 18 h). Thapsigargin and DTT stimulated ATF6 reporter activity, and iPLA$_2\gamma$ amplified the effect of thapsigargin and DTT. *, $p < 0.001$ thapsigargin *versus* untreated (*Vector*); **, $p < 0.05$ DTT *versus* untreated (*Vector*); +, $p < 0.05$ iPLA$_2\gamma$ *versus* vector (Tg); ++, $p < 0.05$ iPLA$_2\gamma$ *versus* vector (DTT), four experiments performed in triplicate.

overexpression of iPLA$_2\gamma$ (Fig. 4, *A–C*). When cells were pre-treated with R-BEL or indomethacin prior to the incubation with tunicamycin, the amplified GRP94 and GRP78 expression was reduced by R-BEL but not by indomethacin (Fig. 4, *D–F*). Thus, iPLA$_2\gamma$ amplifies tunicamycin-induced up-regulation of ER chaperones, and this effect is dependent on iPLA$_2\gamma$ catalytic activity but not on prostanoids.

To verify that endogenous iPLA$_2\gamma$ can also modulate ER chaperone induction, we employed GECs derived from WT and iPLA$_2\gamma$ KO mice. Mouse GECs were incubated with 0.5 or 5 μg/ml tunicamycin for 6 h. iPLA$_2\gamma$ KO cells showed significantly reduced induction of GRP94 and GRP78, compared with WT (Fig. 3, *B–D*), supporting a role for endogenous iPLA$_2\gamma$ in tunicamycin-induced up-regulation of ER chaperones. After 18 h of incubation with tunicamycin, there were large increases in GRP94 and GRP78 expression, such that there were no significant differences between WT and KO GECs (data not shown).

Next, we studied whether comparable effects of iPLA$_2\gamma$ can occur in other cell lines. In COS-1 cells, expression of iPLA$_2\gamma$ amplified tunicamycin-induced up-regulation of GRP94 and

GRP78 (Fig. 5, *A–C*). Furthermore, transfection of iPLA$_2\gamma$ in COS-1 cells independently resulted in a modest but significant increase in ATF6-luciferase reporter activity (Table 2, part A) and, in addition, amplified the tunicamycin-induced stimulation of reporter activity (Table 2, part B). cDNA transfection did not independently stimulate an increase in ATF6-luciferase reporter activity in COS-1 cells (Table 2). In 293T cells, which were reported to express a significant amount of endogenous iPLA$_2\gamma$ (31), tunicamycin induced robust increases in GRP94 and GRP78, and these were reduced substantially when endogenous iPLA$_2\gamma$ was inhibited by R-BEL (Fig. 5, *D–F*). These results are in keeping with the overexpression or deletion of iPLA$_2\gamma$ in GECs and support the role of iPLA$_2\gamma$ in ATF6 activation/ER chaperone induction.

In a previous study, we demonstrated that mutation of serine 511 and serine 515 to alanines partially reduces the catalytic activity of iPLA$_2\gamma$ and that phosphorylation of serine 511 is associated with an increase in activity (11). To address the role of these phosphorylation sites in the activation of ATF6 by iPLA$_2\gamma$, COS-1 cells were transfected with GFP-iPLA$_2\gamma$ (WT) or GFP-iPLA$_2\gamma$ S511A/S515A. As described above, transfec-
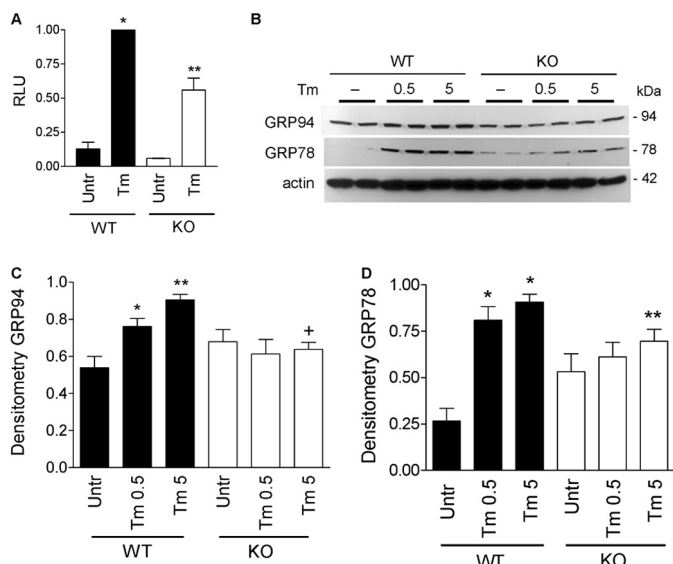
FIGURE 3. **Endogenous iPLA$_2\gamma$ amplifies ATF6 activity and ER chaperones.** *A,* WT and iPLA$_2\gamma$ KO mouse GECs were co-transfected with ATF6 firefly luciferase-reporter and *Renilla* luciferase. Cells were untreated (*Untr*), or incubated with tunicamycin (*Tm,* 0.1 μg/ml, 18 h). Tunicamycin-induced activation of ATF6 reporter was greater in WT cells, compared with iPLA$_2\gamma$ KO. *, $p < 0.001$ Tm *versus* untreated (WT); **, $p < 0.001$ WT *versus* KO (Tm), four experiments performed in triplicate. *RLU,* relative luminescence units. *B,* WT and iPLA$_2\gamma$ KO mouse GECs were untreated or incubated with Tm (0.5 or 5 μg/ml for 6 h). Lysates were immunoblotted with antibodies to GRP94, GRP78, and actin. Tunicamycin increased GRP94 and GRP78 expression levels only in WT podocytes. *B,* representative immunoblots; *C* and *D,* densitometric quantification. *C,* GRP94: *, $p < 0.01$; **, $p < 0.001$ Tm *versus* untreated; +, $p < 0.01$ WT *versus* KO (Tm 5), six experiments performed in duplicate. *D,* GRP78: *, $p < 0.001$ Tm *versus* untreated; **, $p < 0.05$ WT *versus* KO (Tm 5), five experiments performed in duplicate.

tion of GFP-iPLA$_2\gamma$ (WT) independently increased ATF6 response element-luciferase reporter activity, whereas the increase in reporter activity by the S511A/S515A mutant was lower and not significant (Table 2, part C), Experiments to test the role of serine 511 and serine 515 were also performed in GECs (protocol as in Fig. 2*A*). After treating GECs with tunicamycin, expression of GFP-iPLA$_2\gamma$ (WT) enhanced ATF6 luciferase reporter activity by 29%, compared with vector, although expression of GFP-iPLA$_2\gamma$ S511A/S515A increased reporter activity by only 18% (six experiments). These results imply that the enzymatic activity of iPLA$_2\gamma$ is necessary to enhance ATF6 activation.

iPLA$_2\gamma$ Does Not Amplify Tunicamycin-induced PERK and IRE1α Pathway Activation—A second aspect of the UPR involves activation of PERK and phosphorylation of eIF2α. This phosphorylation is associated with a global decrease in translation but preferential translation of *ATF4*, which leads to the induction of several genes, including *CHOP*, a gene closely associated with apoptosis and/or growth arrest (32). We next studied the effect of iPLA$_2\gamma$ on the PERK pathway. Tunicamycin stimulated induction of C/EBP homologous protein-10 (CHOP) in control (vector-transfected) GECs after 6 h (data not shown) or 18 h (Fig. 6, *A* and *B*), but unlike ER chaperones, the stimulation of CHOP was not affected by overexpression of iPLA$_2\gamma$. By analogy, tunicamycin increased CHOP and eIF2α phosphorylation in control COS-1 cells, and the increases in CHOP and eIF2α phosphorylation were not affected by overexpression of iPLA$_2\gamma$ (Fig. 6, *C* and *D*). These results imply that

the PERK pathway is not modulated by iPLA$_2\gamma$. In a third UPR pathway, IRE1α endonuclease activity splices *xbp1* mRNA to yield a potent transcriptional activator. To determine whether IRE1α is modulated by iPLA$_2\gamma$, we monitored *xbp1* splicing by RT-PCR. Tunicamycin (6-h incubation) induced nearly complete splicing of *xbp1* in both vector (control) and iPLA$_2\gamma$-transfected cells (Fig. 6*E*). Complete splicing of *xpb1* was evident in control GECs incubated with tunicamycin for 18 h (data not shown). Overexpression of iPLA$_2\gamma$ did not, however, enhance the *xbp1* splicing (Fig. 6*E*). These results indicate that, similar to PERK, the activation of IRE1α was not modulated by iPLA$_2\gamma$.

iPLA$_2\gamma$ Reduces Tunicamycin-induced Cell Death—The above experiments showed that iPLA$_2\gamma$ amplified tunicamycin-induced expression of ER chaperones in GECs. This aspect of the UPR is typically cytoprotective, because up-regulation of chaperones enhances the protein-folding capacity of the ER. Based on these results, we hypothesized that the amplification of chaperone induction by iPLA$_2\gamma$ is responsible for limiting cell injury. Prolonged incubation of cells with tunicamycin can induce a cytotoxic ER stress response, which is, at least in part, associated with the induction of CHOP (33). Therefore, we examined the effect of iPLA$_2\gamma$ on cytotoxicity during chronic incubation with tunicamycin. Cytotoxicity was monitored by release of LDH (28). Tunicamycin (5–10 μg/ml, 24-h incubation) significantly induced LDH release in control cells, and this was reduced markedly in GECs overexpressing iPLA$_2\gamma$ (Fig. 7), indicating that iPLA$_2\gamma$ is cytoprotective in tunicamycin-induced cell death.

Cytoprotective Effect of iPLA$_2\gamma$ Is Dependent on the ATF6 Pathway—To further investigate whether the cytoprotective effect of iPLA$_2\gamma$ is dependent on ATF6, we employed a cDNA construct that blocks the activity of endogenous ATF6, ATF6(1–373)m1 (ATF6m1). This construct has point mutations in the basic region of ATF6 (KNR to TAA at amino acids 315–317), which are predicted to disrupt the DNA binding activity of the cytoplasmic domain of ATF6, and acts as a dominant negative as it dimerizes with endogenous ATF6 and prevents its binding to ATF6 DNA-binding sites (20). After transfection of GECs with HA-ATF6m1 cDNA, expression of HA-ATF6m1 protein was readily detectable (Fig. 8*A*). As expected, ATF6m1 did not activate the ATF6 reporter and completely inhibited induction of the reporter by tunicamycin (Fig. 8*B*), in keeping with an earlier study (20). Next, we monitored cell death in GECs co-transfected with iPLA$_2\gamma$ and/or ATF6m1. Tunicamycin significantly induced LDH release in vector-transfected control cells (Fig. 8*C*). Consistent with previous results (Fig. 7), iPLA$_2\gamma$ protected against tunicamycin-induced cell death (Fig. 8*C*). The protective effect of iPLA$_2\gamma$ was abolished in cells where iPLA$_2\gamma$ was co-transfected with ATF6m1 (Fig. 8*C*). ATF6m1 alone did not affect tunicamycin-induced cell death. These results indicate that the cytoprotective effect of iPLA$_2\gamma$ during ER stress is dependent on the ATF6 pathway.

To determine whether the protective effect of iPLA$_2\gamma$ on cell death is specifically linked to ER stress or is a general mechanism of cell death, we examined the effect of iPLA$_2\gamma$ on the cytotoxicity of two non-ER stress agents, staurosporine and etoposide. The protocol employed in these experiments was
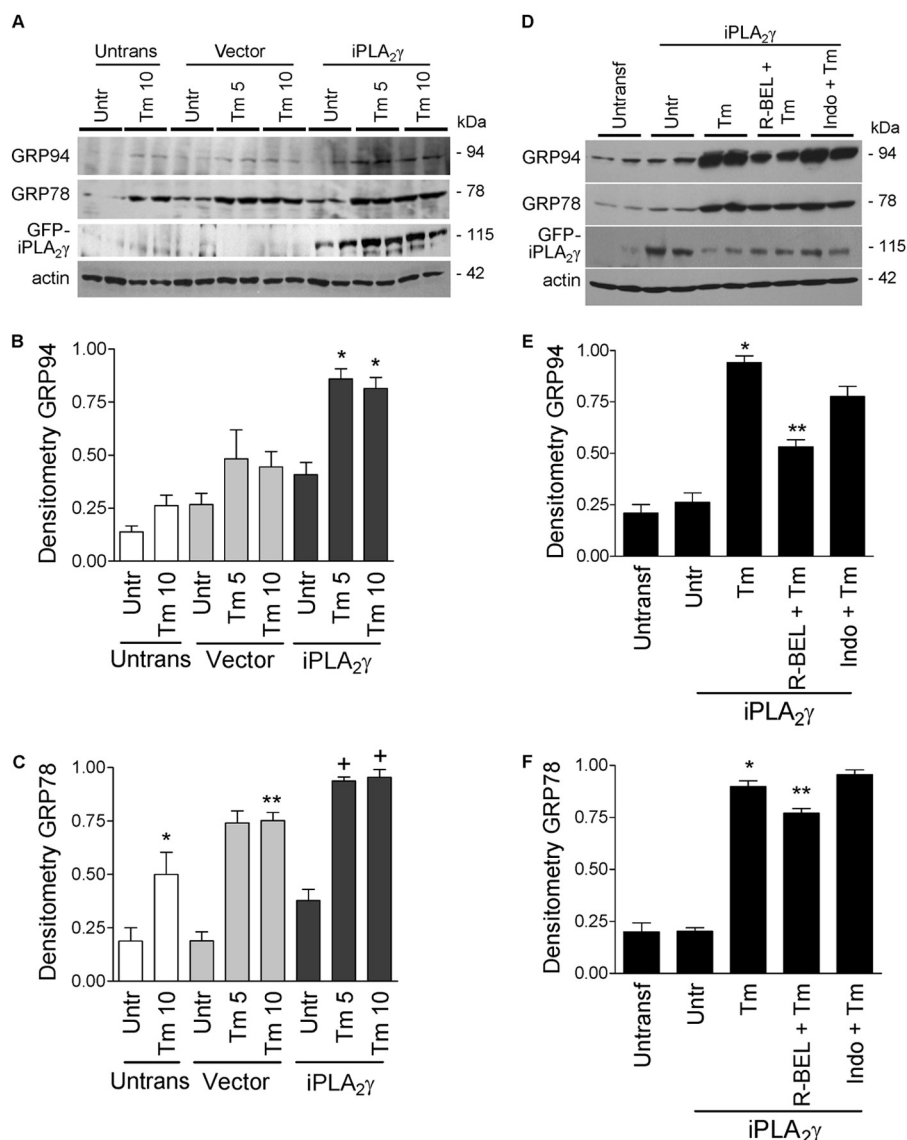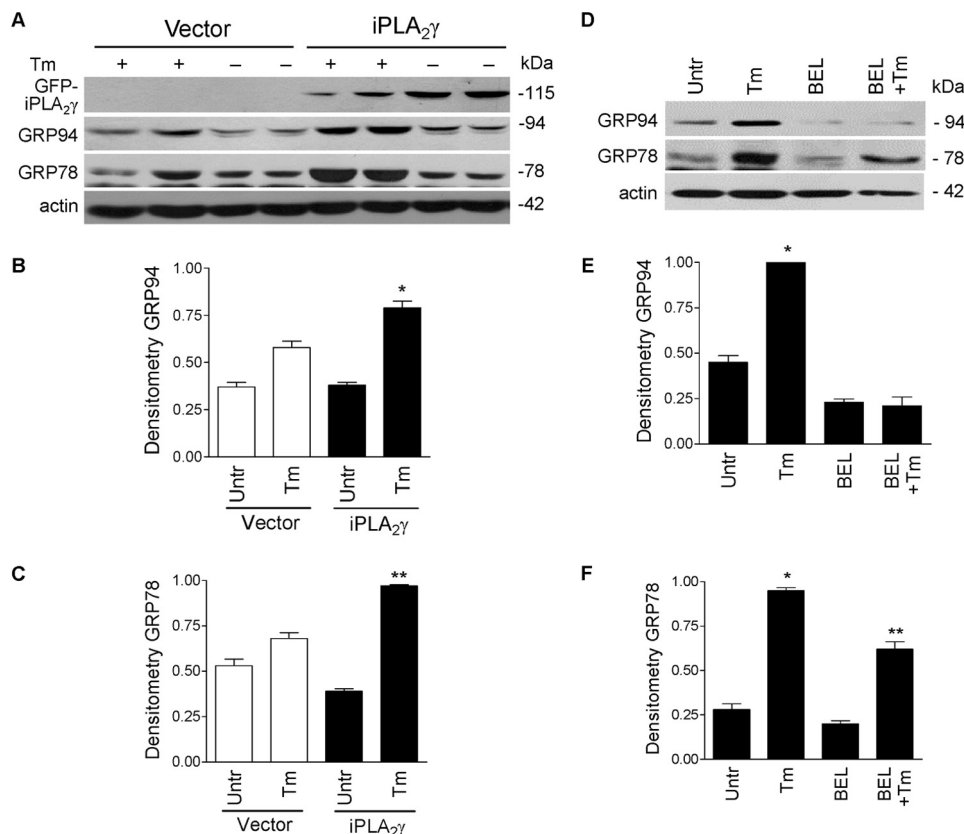
FIGURE 4. **iPLA$_2$γ amplifies the tunicamycin-induced up-regulation of ER chaperones in GECs.** *A–C*, rat GECs were untransfected (*Untrans*) or were transfected with GFP-iPLA$_2$γ or empty vector in control. After 24 h, cells were untreated (*Untr*, or incubated with tunicamycin (*Tm*, 5 or 10 μg/ml, 18 h). Lysates were immunoblotted with antibodies to GRP94, GRP78, GFP (iPLA$_2$γ), and actin. Tunicamycin (5 and 10 μg/ml) tended to increase GRP94 and GRP78 expression levels in untransfected and vector-transfected (control) cells. This effect was amplified by overexpression of iPLA$_2$γ (*A*, representative immunoblots; *B* and *C*, densitometric quantification). *B*, GRP94: *, $p < 0.05$ iPLA$_2$γ *versus* vector (*Tm 5*). *, $p < 0.05$ iPLA$_2$γ *versus* vector (*Tm 10*). *C*, GRP78: *, $p < 0.05$ Tm 10 *versus* untreated (*Untrans*); **, $p < 0.05$ Tm 10 *versus* untreated (*Vector*); +, $p < 0.05$ iPLA$_2$γ *versus* vector (Tm 5 and 10), three experiments performed in duplicate. *D–F*, GECs were untransfected, or were transfected with GFP-iPLA$_2$γ. After 24 h, cells were preincubated with R-BEL (5 μM) or indomethacin (*Indo*, 10 μM) for 30 min. Cells were then treated with Tm (5 μg/ml, 18 h). Lysates were immunoblotted with antibodies to GRP94, GRP78, GFP, and actin. Tunicamycin increased GRP94 and GRP78 expression levels in iPLA$_2$γ-transfected cells. This effect was reduced by R-BEL but not by indomethacin (*D*, representative immunoblots; *E* and *F*, densitometric quantification). *E*, GRP94: *, $p < 0.001$ Tm *versus* untreated. **, $p < 0.001$ R-BEL + Tm *versus* Tm. *F*, GRP78: *, $p < 0.001$ Tm *versus* untreated. **, $p < 0.01$ R-BEL + Tm *versus* Tm, three experiments performed in duplicate.

analogous to the one used in Fig. 7. Incubation of vector-transfected GECs with staurosporine (1 μM) increased LDH release by 19 ± 12% (above values in untreated cells), although the increase in iPLA$_2$γ-transfected GECs was 27 ± 17% (three experiments performed in duplicate). Incubation of vector-transfected GECs with etoposide (300 μM) increased LDH release by 13 ± 6%, although the increase in iPLA$_2$γ-transfected GECs was 20 ± 11% (three experiments performed in duplicate). Thus, unlike the protective effect of iPLA$_2$γ in the cell injury induced by the ER stressor, tunicamycin, no protective effect was evident in injury induced by staurosporine and etoposide.

Effect of iPLA$_2$γ on Sterol Regulatory Element-binding Protein (SREBP)-2—During ER stress, ATF6 is released from the ER and translocates to the Golgi, where it is cleaved by the site-1 and site-2 proteases. The cleaved cytosolic fragment of ATF6 migrates to the nucleus to activate gene transcription. It has been reported that SREBPs are also targets of site-1 and site-2 proteases and that SREBP-2 can be activated by ER stress (34). Alternatively, it was also reported that ATF6 can antagonize SREBP-2 (35). Accordingly, we examined whether iPLA$_2$γ could be involved in the activation of SREBP-2 by ER stress and whether this pathway may be functionally important. First, we tested whether tunicamycin activated the SREBP-2 pathway in

FIGURE 5. **iPLA$_2$γ amplifies the tunicamycin-induced up-regulation of ER chaperones in COS-1 and 293T cells.** *A–C,* COS-1 cells were transfected with GFP-iPLA$_2$γ and were then incubated with tunicamycin (*Tm*, 10 μg/ml, 18 h), as above. Lysates were immunoblotted with antibodies to GRP94, GRP78, GFP, and actin. Tunicamycin tended to increase GRP94 and GRP78 expression levels in control cells. This effect was amplified by overexpression of iPLA$_2$γ (*A,* representative immunoblots; *B* and *C,* densitometric quantification). *B,* GRP94: *, *p* = 0.0015 Tm *versus* untreated (iPLA$_2$γ). *C,* GRP78: *, *p* < 0.0001 Tm *versus* untreated (iPLA$_2$γ). **, *p* = 0.0015 iPLA$_2$γ *versus* vector (Tm), three experiments performed in duplicate. *D–F,* 293T cells were incubated with Tm and/or R-BEL. Lysates were immunoblotted with antibodies to GRP94, GRP78, and actin. Tunicamycin increased GRP94 and GRP78 expression levels. This effect was reduced by R-BEL. *D,* representative immunoblots; *E* and *F,* densitometric quantification. *E,* GRP94: *, *p* < 0.0001 Tm *versus* untreated and Tm *versus* R-BEL + Tm. *F,* GRP78: *, *p* < 0.0001 Tm *versus* untreated and *p* < 0.001 Tm *versus* R-BEL + Tm. **, *p* < 0.001 R-BEL + Tm *versus* R-BEL, three experiments.

TABLE 2

Effect of iPLA$_2$γ on ATF6 luciferase activity in COS-1 cells

Parts A and B, COS-1 cells were untransfected or were transiently co-transfected with M1 GFP-iPLA$_2$γ (WT) or vector (in control), plus ATF6 firefly luciferase-reporter and *Renilla* luciferase. After 24 h, cells were untreated or incubated with tunicamycin (0.1 μg/ml, 24 h). ATF6 reporter activity is expressed in relative luminescence units (RLU). Part C, COS-1 cells were transiently co-transfected with vector, GFP-iPLA$_2$γ (WT), or GFP-iPLA$_2$γ S511A/S515A, plus ATF6 firefly luciferase-reporter and *Renilla* luciferase.

	Transfection/treatment	RLU
A.	Untransfected	1.0
	Vector	1.3 ± 0.2
	GFP-iPLA$_2$γ	3.6 ± 0.8[a]
B.	Untransfected/untreated	1.0
	Untransfected/tunicamycin	16.1 ± 1.4
	Vector/untreated	1.6 ± 0.5
	Vector/tunicamycin	9.3 ± 0.7
	GFP-iPLA$_2$γ/untreated	3.7 ± 1.7
	GFP-iPLA$_2$γ/tunicamycin	27.5 ± 5.9[b]
C.	Vector	1.0
	GFP-iPLA$_2$γ	2.3 ± 0.1[c]
	GFP-iPLA$_2$γ S511A/S515A	1.6 ± 0.3

[a] *p* < 0.001 *versus* vector (four experiments performed in duplicate).
[b] *p* < 0.015 *versus* vector + tunicamycin and *versus* untransfected + tunicamycin (four experiments performed in duplicate).
[c] *p* = 0.005 *versus* vector (four experiments performed in duplicate).

GECs and whether the effect is modulated by iPLA$_2$γ. To monitor SREBP-2-mediated transcription, we used a protocol analogous to the one in Fig. 2, except that we employed a luciferase reporter driven by the LDLR promoter, which contains a SRE

consensus element (LDLR-luciferase) (35). In contrast to the ATF6 response element-luciferase reporter, incubation of GECs with tunicamycin suppressed activation of LDLR-luciferase, and there was no significant modulatory effect of iPLA$_2$γ (Table 3A).

We also examined whether iPLA$_2$γ could modulate the activation of LDLR-luciferase by U18666A, a drug that blocks cholesterol transport from late endosomes and lysosomes to the ER, resulting in depletion of ER membrane cholesterol and activation of SREBP-2 (34). In GECs, U18666A had a modest but significant stimulatory effect on LDLR-luciferase, but iPLA$_2$γ did not enhance the effect of U18666A (Table 3, part B). Together, the results indicate that in GECs, ER stress does not appear to activate SREBP-2, and there is no apparent modulatory role of iPLA$_2$γ in this pathway.

DISCUSSION

In previous studies, we demonstrated that overexpression of iPLA$_2$γ conferred cytoprotection against complement-dependent GEC injury (12) and that full-length iPLA$_2$γ WT is, in part, localized at the ER (11). In this study, we addressed ER stress as a potential mechanism of iPLA$_2$γ-mediated cytoprotection. We demonstrate that in GECs, iPLA$_2$γ amplified the activation of ATF6 and the up-regulation of the ER chaperones, GRP94
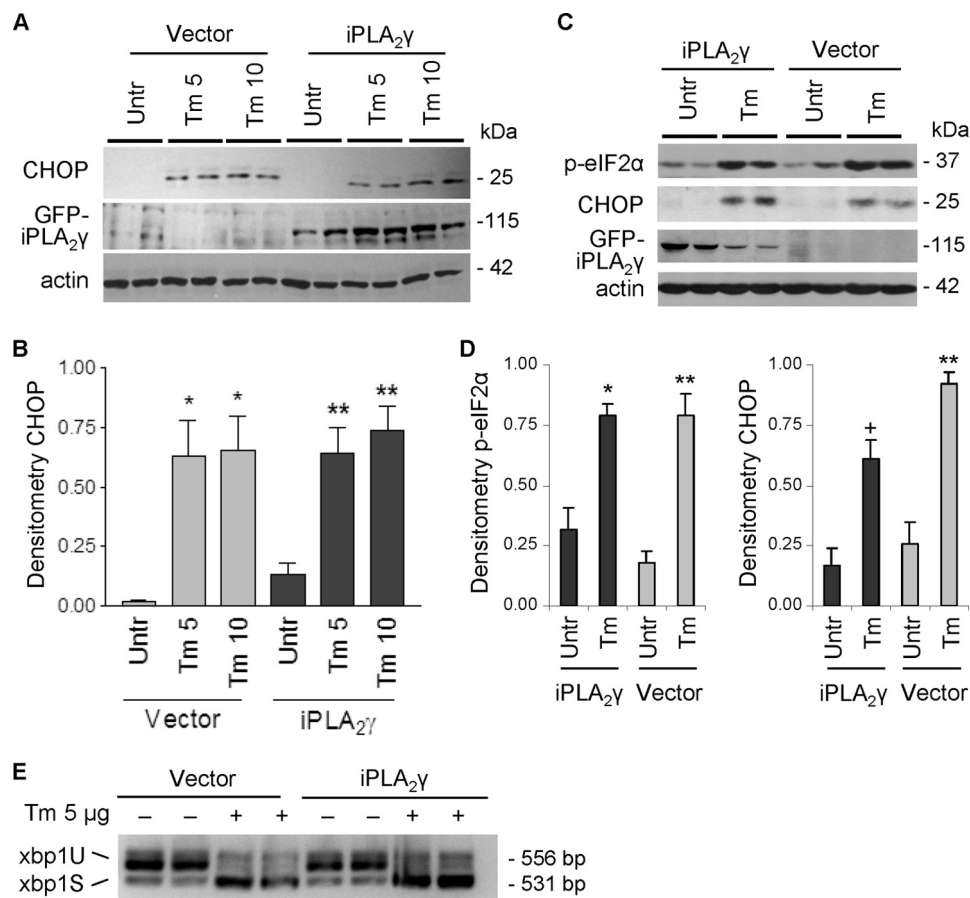
FIGURE 6. **PERK and IRE1α pathways are not modulated by iPLA₂γ during ER stress.** GECs (*A, B,* and *E*) or COS-1 cells (*C* and *D*) were transfected with GFP-iPLA₂γ or empty vector in control. After 24 h, cells were untreated (*Untr*) or were treated with tunicamycin (*Tm,* 5 or 10 μg/ml in GECs; 10 μg/ml in COS-1 cells) for 18 h. *A–D,* lysates were immunoblotted with antibodies to CHOP, phospho (p)-eIF2α, GFP, or actin. Tunicamycin (5 and 10 μg/ml) increased CHOP and phospho-eIF2α in vector-transfected control cells. The stimulation of CHOP or phospho-eIF2α was not affected by iPLA₂γ overexpression. *A* and *C,* representative immunoblots; *B* and *D,* densitometric quantification. *B.* *, $p < 0.001$ Tm 5 and 10 *versus* untreated (*Vector*), **, $p < 0.01$ Tm 5 and 10 *versus* untreated (iPLA₂γ), three experiments performed in duplicate. *D,* *, $p < 0.003$; +, $p < 0.0002$ Tm *versus* untreated (iPLA₂γ); **, $p < 0.0001$ Tm *versus* untreated (*Vector*), 3–4 experiments performed in duplicate. *E,* mRNA was reverse-transcribed, and PCR was conducted to amplify *xbp1* variants. Tunicamycin induced the splicing of 26 bp from *xbp1* in control cells, which reflects activation of IRE1α. Activation of IRE1α was not affected by overexpression of iPLA₂γ.

and GRP78 (Figs. 2 and 4). Conversely, deletion of iPLA₂γ blunted these responses (Fig. 3). Effects of iPLA₂γ on ATF6 and ER chaperones were dependent on iPLA₂γ catalytic activity but not on prostanoids (Fig. 2). Furthermore, full ATF6 amplification occurred only when the full-length iPLA₂γ was expressed, but not an N-terminally truncated mutant, which does not associate with the ER membrane (Fig. 2), or the S511A/S515A mutant (Table 2, part C, and under "Results"). Unlike the ATF6 pathway, the activation of the other two UPR pathways, PERK and IRE1α, was not modulated by iPLA₂γ (Fig. 6). Overexpression of iPLA₂γ in GECs reduced tunicamycin-induced cytotoxicity (Fig. 7). Moreover, the cytoprotective effect iPLA₂γ was reversed by dominant negative ATF6 (Fig. 8). Taken together, the cytoprotective effect of iPLA₂γ during ER stress is dependent on the ATF6 pathway.

To our knowledge, this is the first demonstration that activation of the ATF6 UPR pathway and up-regulation of the ER chaperones can be enhanced via iPLA₂γ catalytic activity. Results obtained in an overexpression system need to be interpreted carefully, because the levels of overexpression could be supra-physiological. Indeed, when tested by quantitative PCR, the iPLA₂γ mRNA level was ~18-fold higher in GECs express-

ing GFP-iPLA₂γ, compared with control GECs transfected with vector (Table 1). However, when iPLA₂ enzymatic activities in cell lysates were previously compared between transfected and control cells, using an *in vitro* assay, the difference was only ~2-fold (11). Similarly, prostaglandin E₂ production between vector- and GFP-iPLA₂γ-transfected GECs increased ~2-fold (11), implying that ectopic iPLA₂γ was expressed at twice the level of endogenous iPLA₂γ. These results suggest that iPLA₂γ mRNA is not translated efficiently into catalytically active enzyme, and the total amount of iPLA₂γ activity in GECs was most likely within the physiological range. Furthermore, the results with overexpression were supported by complementary experiments, which employed the iPLA₂γ inhibitor, R-BEL, and iPLA₂γ KO cells. Both approaches demonstrated analogous actions of endogenous iPLA₂γ, strengthening the conclusion that iPLA₂γ amplifies the induction of ER chaperones via ATF6 activation. It remains to be determined, however, if the iPLA₂γ expression level is regulated in GECs under various pathological conditions. By analogy to GECs, the role of iPLA₂γ in the induction of ER stress was confirmed in COS-1 and 293T cells (Fig. 5 and Table 2). Thus, the role of iPLA₂γ in ER stress was not restricted to a single cell type.

iPLA$_2\gamma$ Enhances Activation of ATF6

We and others have shown functional coupling of iPLA$_2\gamma$ with cyclooxygenases, as activation of iPLA$_2\gamma$ results in release of arachidonic acid and production of prostanoids (12, 31). In this study, we demonstrated that the effect of iPLA$_2\gamma$ on tunicamycin-mediated activation of ATF6 and up-regulation of ER chaperones was, however, independent of prostanoids (Fig. 2). Therefore, the cytoprotective effect of iPLA$_2\gamma$ in the model of tunicamycin-induced cell death would probably also be prostanoid-independent. In contrast, cytoprotection by iPLA$_2\gamma$ against complement-induced GEC injury was partially reversed by indomethacin, suggesting that it was at least in part mediated by prostanoids (12). Most likely, iPLA$_2\gamma$ exerts cytoprotection via cyclooxygenase-dependent and -independent mechanisms depending on the cell type and context. In this study, the cytoprotective effect of iPLA$_2\gamma$ was associated with the activation of ATF6 (Fig. 8). Cleaved ATF6 can activate transcription of multiple genes (36). A number of these are chaperones or factors within chaperone pathways, including BiP, GRP94, heat shock protein-40, calreticulin, ATF4, XBP1, and others. Up-regulation of such genes potentially enhances the chaperoning capacity of a cell, thereby alleviating adverse effects of protein misfolding and reducing cytotoxicity. Furthermore, it should also be considered that mechanisms other than ATF6 activation at the ER could contribute to iPLA$_2\gamma$ cytoprotection; for example, the action of iPLA$_2\gamma$ could involve reducing lipid peroxidation (4, 6). In GECs, a portion of iPLA$_2\gamma$ was localized at the mitochondria (11). Thus, by analogy to its action in kidney cortical preparations, iPLA$_2\gamma$ may protect GEC mitochondria from oxidant-induced lipid peroxidation and dysfunction (37).

Similarly to iPLA$_2\gamma$, iPLA$_2\beta$ was protective in complement-mediated cellular injury (12). In contrast, cytotoxic effects of PLA$_2$s have also been described. Secretory PLA$_2$s facilitate various forms of inflammatory tissue injury. Cytosolic PLA$_2\alpha$ was shown to exacerbate cell death induced by complement and hydrogen peroxide and was reported to disrupt the structure of cellular organelles (28, 38). At the same time cytosolic PLA$_2\alpha$ enhanced the activation of a cytoprotective UPR, which attenuated cytotoxicity (28). Both cytosolic PLA$_2\alpha$ and iPLA$_2\beta$ were
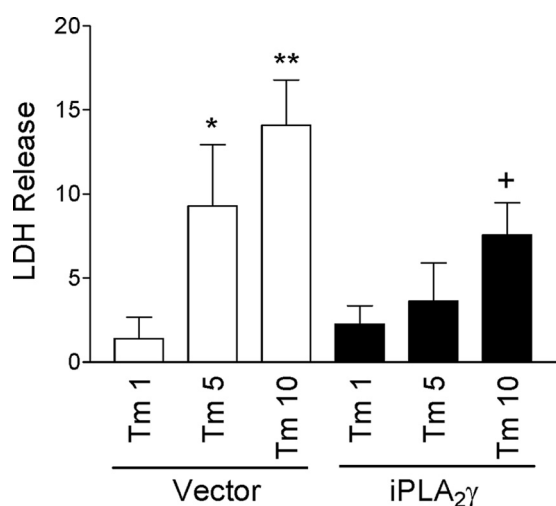
FIGURE 7. **iPLA$_2\gamma$ reduced tunicamycin-induced cell death.** GECs were transfected with GFP-iPLA$_2\gamma$ or empty vector in control. After 24 h, cells were untreated or were treated with tunicamycin (*Tm*, 1, 5, or 10 μg/ml) for 24 h. Tunicamycin-induced cytotoxicity was monitored by LDH release. The results show Tm-induced LDH release above the values in untreated cells. Tunicamycin (5 and 10 μg/ml) significantly induced LDH release in vector-transfected cells. This effect was reduced in GECs overexpressing iPLA$_2\gamma$. *, $p < 0.05$; **, $p < 0.01$ Tm *versus* untreated (*Vector*). +, $p < 0.01$ iPLA$_2\gamma$ *versus* vector (Tm 10), five experiments performed in duplicate.

TABLE 3

Effect of iPLA$_2\gamma$ on LDLR promoter-luciferase reporter activity in GECs

Parts A and B, GECs were untransfected or were transiently co-transfected with GFP-iPLA$_2\gamma$ (WT) or vector (in control), plus LDLR promoter firefly luciferase-reporter and *Renilla* luciferase. After 24 h, cells were untreated (Untr) or incubated with tunicamycin (0.1 μg/ml, 18 h; part A) or U18666A (2 μg/ml, 18 h; part B). LDLR reporter activity is expressed in relative luminescence units (RLU). Tunicamycin did not stimulate LDLR reporter activity (four experiments performed in triplicate). Although U18666A stimulated LDLR reporter activity, there was no enhancement of this effect by iPLA$_2\gamma$.

	Transfection/Treatment		RLU
A.	Vector	Untreated	0.67 ± 0.18
		Tunicamycin	0.24 ± 0.08
	iPLA$_2\gamma$	Untreated	0.95 ± 0.05
		Tunicamycin	0.31 ± 0.04
B.	Vector	Untreated	0.75 ± 0.06
		U18666A	1.00 ± 0.00[a]
	iPLA$_2\gamma$	Untreated	0.45 ± 0.05
		U18666A	0.50 ± 0.09

[a] $p = 0.04$ *versus* vector/untreated (four experiments performed in triplicate).
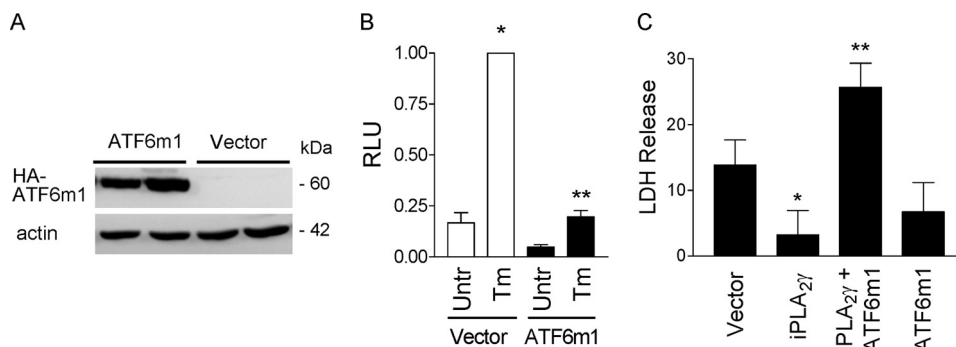
FIGURE 8. **Cytoprotective effect of iPLA$_2\gamma$ during ER stress is dependent on the ATF6 pathway.** GECs were transiently transfected with HA-ATF6m1 (dominant negative ATF6) or empty vector. *A*, lysates were immunoblotted with antibody to HA. ATF6m1 expression is presented. *B*, GECs were transiently co-transfected with ATF6m1 or vector in control, plus ATF6 firefly luciferase-reporter and *Renilla* luciferase. Cells were untreated (*Untr*), or incubated with Tm (0.1 μg/ml, 18 h). ATF6m1 completely inhibited stimulated ATF6 reporter activity. *, $p < 0.001$ Tm *versus* untreated (*Vector*); **, $p < 0.001$ ATF6m1 *versus* vector (Tm), two experiments performed in duplicate. *RLU*, relative luminescence units. *C*, GECs were transfected with vector, iPLA$_2\gamma$, ATF6m1, or iPLA$_2\gamma$ + ATF6m1. After 24 h, cells were untreated or were treated with tunicamycin (*Tm*, 10 μg/ml) for 24 h. The results show Tm-induced LDH release above the values in untreated cells. Tunicamycin induced significant LDH release in vector-transfected control cells. Overexpression of iPLA$_2\gamma$ attenuated the Tm-induced release of LDH. The cytoprotective effect iPLA$_2\gamma$ was reversed by ATF6m1. *, $p < 0.05$ iPLA$_2\gamma$ *versus* vector (Tm); **, $p < 0.01$ iPLA$_2\gamma$ + ATF6m1 *versus* iPLA$_2\gamma$ (Tm), five experiments performed in duplicate.

implicated in promoting or reducing apoptotic cell death, respectively (38). These complex and apparently conflicting effects of the PLA$_2$ isoforms could be related to the subcellular localization of the enzymes and their site of activation, as well as the temporal activation pattern during the course of cell injury. Moreover, the effects of the PLA$_2$s may be directly due to PLA$_2$-mediated phospholipid hydrolysis/remodeling or associated with the production of pro- or anti-inflammatory mediators from arachidonic acid or lysophospholipid release (38).

The mechanism(s) by which iPLA$_2$γ stimulated ATF6 could potentially involve ER membrane lipids. Perturbation of cellular lipid composition was shown to activate the UPR in several cells. For example, UPR signaling was enhanced in cholesterol-loaded macrophages (39), in liver of mice fed a high fat diet (40), and in pancreatic beta cells exposed to saturated fatty acids (41). The precise biochemical mechanisms by which perturbation of the cellular lipid activates UPR pathways in these cells remain unknown. It was proposed that altered membrane lipid composition may potentially alter Ca^{2+} homeostasis by inhibition of the sarco/endoplasmic reticulum calcium ATPase (40). This may lead to Ca^{2+} depletion from the ER, which in turn activates the UPR by interfering with Ca^{2+}-dependent chaperones and enzymes required for protein folding (40). Alternatively, direct sensing of lipid perturbation may contribute to activation of ATF6. For example, perturbation of the lipid bilayer of the ER by the expression of a tail-anchored ER membrane protein resulted in the selective activation of ATF6, in the absence of IRE1α and PERK activation (and without ER Ca^{2+} depletion) (42). Conversely, a recent study has demonstrated that saturation of membrane lipids promoted selective IRE1α and PERK activation by enhancing dimerization via their transmembrane domains (43). Defining the precise mechanism of ATF6 activation by iPLA$_2$γ will require further investigation.

In conclusion, the results of this study demonstrate a key relationship between iPLA$_2$γ and ATF6 activation. Additionally, we have shown that iPLA$_2$γ plays a cytoprotective role involving the ATF6 pathway of the UPR. Stimulation of iPLA$_2$γ enzymatic activity represents a potentially novel approach to limiting GEC injury in proteinuric glomerular diseases.

REFERENCES

1. Murakami, M., and Kudo, I. (2002) Phospholipase A2. *J. Biochem.* **131,** 285–292
2. Six, D. A., and Dennis, E. A. (2000) The expanding superfamily of phospholipase A(2) enzymes: classification and characterization. *Biochim. Biophys. Acta* **1488,** 1–19
3. Funk, C. D. (2001) Prostaglandins and leukotrienes: advances in eicosanoid biology. *Science* **294,** 1871–1875
4. Cummings, B. S., McHowat, J., and Schnellmann, R. G. (2002) Role of an endoplasmic reticulum Ca^{2+}-independent phospholipase A(2) in oxidant-induced renal cell death. *Am. J. Physiol. Renal Physiol.* **283,** F492–F498
5. Mancuso, D. J., Jenkins, C. M., Sims, H. F., Cohen, J. M., Yang, J., and Gross, R. W. (2004) Complex transcriptional and translational regulation of iPLA γ resulting in multiple gene products containing dual competing sites for mitochondrial or peroxisomal localization. *Eur. J. Biochem.* **271,** 4709–4724
6. Kinsey, G. R., Blum, J. L., Covington, M. D., Cummings, B. S., McHowat, J., and Schnellmann, R. G. (2008) Decreased iPLA2γ expression induces lipid peroxidation and cell death and sensitizes cells to oxidant-induced apoptosis. *J. Lipid Res.* **49,** 1477–1487
7. Cummings, B. S., McHowat, J., and Schnellmann, R. G. (2004) Role of an endoplasmic reticulum Ca^{2+}-independent phospholipase A2 in cisplatin-induced renal cell apoptosis. *J. Pharmacol. Exp. Ther.* **308,** 921–928
8. Gadd, M. E., Broekemeier, K. M., Crouser, E. D., Kumar, J., Graff, G., and Pfeiffer, D. R. (2006) Mitochondrial iPLA2 activity modulates the release of cytochrome *c* from mitochondria and influences the permeability transition. *J. Biol. Chem.* **281,** 6931–6939
9. Mancuso, D. J., Kotzbauer, P., Wozniak, D. F., Sims, H. F., Jenkins, C. M., Guan, S., Han, X., Yang, K., Sun, G., Malik, I., Conyers, S., Green, K. G., Schmidt, R. E., and Gross, R. W. (2009) Genetic ablation of calcium-independent phospholipase A$_2$γ leads to alterations in hippocampal cardiolipin content and molecular species distribution, mitochondrial degeneration, autophagy, and cognitive dysfunction. *J. Biol. Chem.* **284,** 35632–35644
10. Mancuso, D. J., Sims, H. F., Yang, K., Kiebish, M. A., Su, X., Jenkins, C. M., Guan, S., Moon, S. H., Pietka, T., Nassir, F., Schappe, T., Moore, K., Han, X., Abumrad, N. A., and Gross, R. W. (2010) Genetic ablation of calcium-independent phospholipase A$_2$γ prevents obesity and insulin resistance during high fat feeding by mitochondrial uncoupling and increased adipocyte fatty acid oxidation. *J. Biol. Chem.* **285,** 36495–36510
11. Elimam, H., Papillon, J., Takano, T., and Cybulsky, A. V. (2013) Complement-mediated activation of calcium-independent phospholipase A$_2$γ: role of protein kinases and phosphorylation. *J. Biol. Chem.* **288,** 3871–3885
12. Cohen, D., Papillon, J., Aoudjit, L., Li, H., Cybulsky, A. V., and Takano, T. (2008) Role of calcium-independent phospholipase A$_2$ in complement-mediated glomerular epithelial cell injury. *Am. J. Physiol. Renal Physiol.* **294,** F469–F479
13. Araki, K., and Nagata, K. (2011) Protein folding and quality control in the ER. *Cold Spring Harb. Perspect. Biol.* **3,** a007526
14. Ron, D., and Walter, P. (2007) Signal integration in the endoplasmic reticulum unfolded protein response. *Nat. Rev. Mol. Cell Biol.* **8,** 519–529
15. Yoshida, H. (2007) ER stress and diseases. *FEBS J.* **274,** 630–658
16. Hetz, C. (2012) The unfolded protein response: controlling cell fate decisions under ER stress and beyond. *Nat. Rev. Mol. Cell Biol.* **13,** 89–102
17. Zhang, K., and Kaufman, R. J. (2008) From endoplasmic-reticulum stress to the inflammatory response. *Nature* **454,** 455–462
18. Cybulsky, A. V. (2013) The intersecting roles of endoplasmic reticulum stress, ubiquitin- proteasome system, and autophagy in the pathogenesis of proteinuric kidney disease. *Kidney Int.* **84,** 25–33
19. Rutkowski, D. T., and Hegde, R. S. (2010) Regulation of basal cellular physiology by the homeostatic unfolded protein response. *J. Cell Biol.* **189,** 783–794
20. Wang, Y., Shen, J., Arenzana, N., Tirasophon, W., Kaufman, R. J., and Prywes, R. (2000) Activation of ATF6 and an ATF6 DNA binding site by the endoplasmic reticulum stress response. *J. Biol. Chem.* **275,** 27013–27020
21. Castoreno, A. B., Wang, Y., Stockinger, W., Jarzylo, L. A., Du, H., Pagnon, J. C., Shieh, E. C., and Nohturfft, A. (2005) Transcriptional regulation of phagocytosis-induced membrane biogenesis by sterol regulatory element binding proteins. *Proc. Natl. Acad. Sci. U.S.A.* **102,** 13129–13134
22. Jat, P. S., Noble, M. D., Ataliotis, P., Tanaka, Y., Yannoutsos, N., Larsen, L., and Kioussis, D. (1991) Direct derivation of conditionally immortal cell lines from an H-2Kb-tsA58 transgenic mouse. *Proc. Natl. Acad. Sci. U.S.A.* **88,** 5096–5100
23. Coers, W., Reivinen, J., Miettinen, A., Huitema, S., Vos, J. T., Salant, D. J., and Weening, J. J. (1996) Characterization of a rat glomerular visceral epithelial cell line. *Exp. Nephrol.* **4,** 184–192
24. Mancuso, D. J., Sims, H. F., Han, X., Jenkins, C. M., Guan, S. P., Yang, K., Moon, S. H., Pietka, T., Abumrad, N. A., Schlesinger, P. H., and Gross, R. W. (2007) Genetic ablation of calcium-independent phospholipase A$_2$γ leads to alterations in mitochondrial lipid metabolism and function result-

ing in a deficient mitochondrial bioenergetic phenotype. *J. Biol. Chem.* **282,** 34611–34622

25. Mundel, P., Reiser, J., and Kriz, W. (1997) Induction of differentiation in cultured rat and human podocytes. *J. Am. Soc. Nephrol.* **8,** 697–705

26. Saleem, M. A., O'Hare, M. J., Reiser, J., Coward, R. J., Inward, C. D., Farren, T., Xing, C. Y., Ni, L., Mathieson, P. W., and Mundel, P. (2002) A conditionally immortalized human podocyte cell line demonstrating nephrin and podocin expression. *J. Am. Soc. Nephrol.* **13,** 630–638

27. Mundel, P., Reiser, J., Zúñiga Mejía Borja, A., Pavenstädt, H., Davidson, G. R., Kriz, W., and Zeller, R. (1997) Rearrangements of the cytoskeleton and cell contacts induce process formation during differentiation of conditionally immortalized mouse podocyte cell lines. *Exp. Cell Res.* **236,** 248–258

28. Cybulsky, A. V., Takano, T., Papillon, J., Khadir, A., Liu, J., and Peng, H. (2002) Complement C5b-9 membrane attack complex increases expression of endoplasmic reticulum stress proteins in glomerular epithelial cells. *J. Biol. Chem.* **277,** 41342–41351

29. Lytton, J., Westlin, M., and Hanley, M. R. (1991) Thapsigargin inhibits the sarcoplasmic or endoplasmic reticulum Ca-ATPase family of calcium pumps. *J. Biol. Chem.* **266,** 17067–17071

30. Ren, G., Takano, T., Papillon, J., and Cybulsky, A. V. (2010) Cytosolic phospholipase A$_2$-α enhances induction of endoplasmic reticulum stress. *Biochim. Biophys. Acta* **1803,** 468–481

31. Murakami, M., Masuda, S., Ueda-Semmyo, K., Yoda, E., Kuwata, H., Takanezawa, Y., Aoki, J., Arai, H., Sumimoto, H., Ishikawa, Y., Ishii, T., Nakatani, Y., and Kudo, I. (2005) Group VIB Ca^{2+}-independent phospholipase A$_2\gamma$ promotes cellular membrane hydrolysis and prostaglandin production in a manner distinct from other intracellular phospholipases A$_2$. *J. Biol. Chem.* **280,** 14028–14041

32. Zinszner, H., Kuroda, M., Wang, X., Batchvarova, N., Lightfoot, R. T., Remotti, H., Stevens, J. L., and Ron, D. (1998) CHOP is implicated in programmed cell death in response to impaired function of the endoplasmic reticulum. *Genes Dev.* **12,** 982–995

33. Cybulsky, A. V., Takano, T., Papillon, J., Kitzler, T. M., and Bijian, K. (2011) Endoplasmic reticulum stress in glomerular epithelial cell injury. *Am. J. Physiol. Renal Physiol.* **301,** F496–F508

34. Lhoták, S., Sood, S., Brimble, E., Carlisle, R. E., Colgan, S. M., Mazzetti, A., Dickhout, J. G., Ingram, A. J., and Austin, R. C. (2012) ER stress contributes to renal proximal tubule injury by increasing SREBP-2-mediated lipid accumulation and apoptotic cell death. *Am. J. Physiol. Renal Physiol.* **303,** F266–F278

35. Zeng, L., Lu, M., Mori, K., Luo, S., Lee, A. S., Zhu, Y., and Shyy, J. Y. (2004) ATF6 modulates SREBP2-mediated lipogenesis. *EMBO J.* **23,** 950–958

36. Belmont, P. J., Chen, W. J., San Pedro, M. N., Thuerauf, D. J., Gellings Lowe, N., Gude, N., Hilton, B., Wolkowicz, R., Sussman, M. A., and Glembotski, C. C. (2010) Roles for endoplasmic reticulum-associated degradation and the novel endoplasmic reticulum stress response gene Derlin-3 in the ischemic heart. *Circ. Res.* **106,** 307–316

37. Kinsey, G. R., McHowat, J., Beckett, C. S., and Schnellmann, R. G. (2007) Identification of calcium-independent phospholipase A$_2\gamma$ in mitochondria and its role in mitochondrial oxidative stress. *Am. J. Physiol. Renal Physiol.* **292,** F853–F860

38. Cummings, B. S., McHowat, J., and Schnellmann, R. G. (2000) Phospholipase A(2)s in cell injury and death. *J. Pharmacol. Exp. Ther.* **294,** 793–799

39. Feng, B., Yao, P. M., Li, Y., Devlin, C. M., Zhang, D., Harding, H. P., Sweeney, M., Rong, J. X., Kuriakose, G., Fisher, E. A., Marks, A. R., Ron, D., and Tabas, I. (2003) The endoplasmic reticulum is the site of cholesterol-induced cytotoxicity in macrophages. *Nat. Cell Biol.* **5,** 781–792

40. Fu, S., Yang, L., Li, P., Hofmann, O., Dicker, L., Hide, W., Lin, X., Watkins, S. M., Ivanov, A. R., and Hotamisligil, G. S. (2011) Aberrant lipid metabolism disrupts calcium homeostasis causing liver endoplasmic reticulum stress in obesity. *Nature* **473,** 528–531

41. Cunha, D. A., Hekerman, P., Ladrière, L., Bazarra-Castro, A., Ortis, F., Wakeham, M. C., Moore, F., Rasschaert, J., Cardozo, A. K., Bellomo, E., Overbergh, L., Mathieu, C., Lupi, R., Hai, T., Herchuelz, A., Marchetti, P., Rutter, G. A., Eizirik, D. L., and Cnop, M. (2008) Initiation and execution of lipotoxic ER stress in pancreatic beta-cells. *J. Cell Sci.* **121,** 2308–2318

42. Maiuolo, J., Bulotta, S., Verderio, C., Benfante, R., and Borgese, N. (2011) Selective activation of the transcription factor ATF6 mediates endoplasmic reticulum proliferation triggered by a membrane protein. *Proc. Natl. Acad. Sci. U.S.A.* **108,** 7832–7837

43. Volmer, R., van der Ploeg, K., and Ron, D. (2013) Membrane lipid saturation activates endoplasmic reticulum unfolded protein response transducers through their transmembrane domains. *Proc. Natl. Acad. Sci. U.S.A.* **110,** 4628–4633